Computational Fluid Dynamics Analysis and Verification of Hydraulic Performance in Drip Irrigation Emitters

Li Yongxin[1]; Li Guangyong[2]; Qiu Xiangyu[3]; Wang Jiandong[4]; Mahbub Alam[5]

Abstract:

The Computational Fluid Dynamics (CFD) method was applied to investigate the hydraulic performance of labyrinth type emitter. The characteristic of the emitter (COE), the relationship between the flow rate of the emitter and the pipe pressure, was numerically calculated using CFD model, and the standard k– ε turbulence model was introduced in the calculation. The modeling results were compared with the laboratory test results. The CFD modeling results show a good correlation with measured results. The pressure and velocity distributions in the flow path of the labyrinth emitter were numerically simulated by the CFD method, and were compared to the pressure distribution obtained from a prototype of the emitter manufactured with the dimensional ratio of 10:1. Both modeling and the measured results indicated that the pressure was reduced linearly with the length of the emitter flow path. The CFD method was found to be an effective method to investigate the hydrodynamic performance of drip emitters.

Introduction:

The emitter is an important component in a drip irrigation system. As water flows into the emitter from the lateral pipe, the turbulent flow path of the emitter dissipates energy and thereby reduces pressure. Ordinarily, the emitter flowrate increases with the static pressure in a lateral pipe in an exponential relation (Karmelli, 1977). The relationship between the emitter flowrate and the static pressure of the pipe, which is called characteristic of emitters (COE), is very important to a drip irrigation system. This relationship is used in designing the desired emitter flow path. Computational Fluid Dynamics (CFD) numerical technique was applied to investigate the flow, heat and mass transfer for many years. CFD technique has many advantages compared with other numerical calculation methods. The simulation can maintain a stable boundary condition while CFD modeling can be easily simulated with the change of the structure specification (Lee and Short, 2000). The numerical calculation results can help researcher analyze the hydraulic performance of the emitters and modify the geometries of the flow path, thus reducing time and cost for producing new emitter designs (P. Salvador et al, 2004).

The objective of this study was to apply the Computational Fluid Dynamics (CFD) numerical method to investigate the hydraulic performance of drip irrigation emitters, and to simulate the

[1] Associate Professor, Department of Fluid Machinery & Fluid Engineering, China Agricultural University, Beijing 100083, China.

[2] Professor, Department of Irrigation and Drainage Engineering, China Agricultural University, Beijing 100083, China. E-mail: lgyl@cau.edu.cn

[3] Masters Candidate, Dept. of Irrigation and Drainage, China Agricultural University.

[4] Masters Candidate, Dept. of Irrigation and Drainage, China Agricultural University.

[5] Associate Professor, Biological and Agricultural Engineering, Kansas State University, Kansas, USA.

distributions of pressure and velocity in the flow path of the labyrinth emitter. The CFD modeling results are validated by measuring results in the laboratory.

Materials and Methods

Labyrinth Emitters

An emitter with standard labyrinth flow path was selected for this study. There are many zigzag teeth on both sides of the emitter (Figure 1), and the space among the teeth forms the flow path of the emitter. The length of flow path for the emitter was 19.8 mm, the depth of the flow path was 0.7 mm, and the distance between the teeth was 1.5 mm.

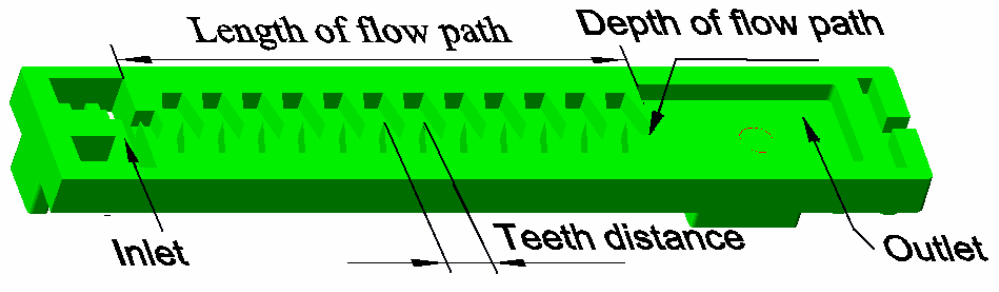

Figure 1 Structure of the labyrinth emitters

CFD Numerical Modeling

The CFD method divides the calculation domain into finite control volumes, and numerically solves the Reynolds–averaged form of the Navier–Stokes equations (Fluent, 1998) within the volumes. The Reynolds–averaged form considers the instantaneous flow parameters as the sum of a mean and a fluctuating component of turbulence (Hinze, 1975; Bennet and Myers, 1995). Since the high–frequency and small–scale fluctuations of turbulent flow could not be directly quantified; turbulence numerical modeling relates some or all of the turbulent velocity fluctuations to the mean flow quantities and their gradients.

1. The water flow inside the emitter was assumed to be an incompressible steady flow. The governing equation included the following continuity equation and Navier-stokes equation (Anderson, 1995):

2. Continuity equation:
$$\frac{\partial u}{\partial x}+\frac{\partial v}{\partial y}+\frac{\partial w}{\partial z}=0$$

3. Navier-Stokes equation：
$$\frac{\partial(\rho u)}{\partial t}+\nabla\cdot(\rho uU)=-\frac{\partial p}{\partial x}+\mu\nabla^2 u+\rho f_x$$
$$\frac{\partial(\rho v)}{\partial t}+\nabla\cdot(\rho vU)=-\frac{\partial p}{\partial y}+\mu\nabla^2 v+\rho f_y$$
$$\frac{\partial(\rho w)}{\partial t}+\nabla\cdot(\rho wU)=-\frac{\partial p}{\partial z}+\mu\nabla^2 w+\rho f_z$$

4. Where U is the flow velocity：$U=u\vec{i}+v\vec{j}+w\vec{k}$ （ms^{-1}），u，v，w are the components of the velocity vector in x，y，z axis; ρ (kg m^{-3}) and μ (Pa s) are the density and dynamic viscosity coefficient of the fluid. The pressure of the fluid is p (Pa); f_x f_y f_z are

the components of the body force.

5. There are two flow patterns in the flow path, laminar flow and turbulence flow, which can be discriminated by Reynolds Number of the flow. But the flow path in emitters is so complicated that the signs of turbulence flow appear with low Reynolds Number. In this study, the standard k– ε turbulence model was selected to describe the flow in emitters because its results were very close to the practical flows (Launder and Spalding, 1974). In the k– ε model, the turbulent kinetic energy (k) and the dissipation rate of (ε) can be expressed as the following equations:

$$k = \frac{1}{2}(\overline{u'^2} + \overline{v'^2} + \overline{w'^2})$$

$$\varepsilon = \nu(\overline{\frac{\partial u_i'}{\partial x_k}}\overline{(\frac{\partial u_i'}{\partial x_k})})$$

Where u'、v'、w'（ms^{-1}）are the fluctuating components of the velocity, ν ($m^2\ s^{-1}$) is the kinematics viscosity coefficient of the fluid. In the standard k– ε turbulence model, the transport equations of the turbulent kinetic energy (k) and the dissipation rate of (ε) are:

Where μ_T is turbulent eddy viscosity, G_k represents the generation of turbulence kinetic energy

$$\frac{\partial}{\partial t}(\rho k) + \frac{\partial}{\partial x_i}(\rho k U) = \frac{\partial}{\partial x_i}[(\mu + \frac{\mu_t}{\sigma_k}\frac{\partial k}{\partial x_i})] + G_k + G_b - \rho\varepsilon - Y_M$$

$$\frac{\partial}{\partial t}(\rho\varepsilon) + \frac{\partial}{\partial x_i}(\rho\varepsilon U) = \frac{\partial}{\partial x_i}[(\mu + \frac{\mu_t}{\sigma_\varepsilon}\frac{\partial \varepsilon}{\partial x_i})] + C_{1\varepsilon}\frac{\varepsilon}{k}(G_k + C_{3\varepsilon}G_b) - C_{2\varepsilon}\rho\frac{\varepsilon^2}{k}$$

caused by the mean velocity gradients, G_b is the generation of turbulence kinetic energy caused by buoyancy, Y_M represents the contribution of the fluctuating dilatation in compressible turbulence to the overall dissipation rate, and $C_{1\varepsilon}$、$C_{2\varepsilon}$、$C_{3\varepsilon}$、σ_k、σ_ε are the turbulent Prandtl numbers for k and ε respectively.

6. The grid generation is very important in CFD numerical calculation. The hexahedron cells with 0.1 mm were applied to generate the grid, and the cell number in the domain of the flow path of the emitter was about 10^5 (figure 2).

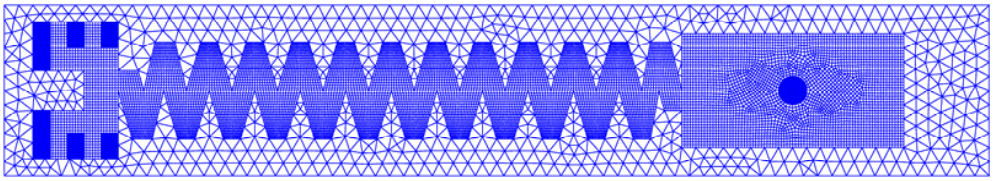

Figure 2. Grid generation of the labyrinth emitter

After completing the grid generation, a grid file was created and fed as input into FLUENT. The boundary conditions were set in FLUENT according to the practical flow situation. The inlet of the emitter was set as a pressure-inlet boundary condition, and was directed into with 3m, 5m, 8m, 10m, 12m, 15m, 18m, and 20m water heads respectively. The outlet of the emitter was set as a pressure-outlet boundary condition; the local atmospheric pressure was included in the calculation as the operational condition.

The local Reynolds number in the boundary layer region near the walls was so small that viscous effects were predominant over turbulent effects. Two methods were used to account for this effect and for the large gradients of variables near the wall; one method applied the wall function to solve the flow near the wall, another method improved the turbulence model to solve the problem. The wall function method, with low calculation load and high accuracy, was applied extensively in the practical engineering calculations. In this study, the standard wall function was applied in the region near the wall, and the roughness of the wall inside the emitter was set as 0.01 mm, which is the ordinary technology level of plastic molding.

Measurement Procedure

The measurements were conducted in the laboratory of irrigation and drainage in China Agricultural University. The measurements included two parts: the COE measuring and the measuring of pressure inside an amplifying model.

The emitters are always integrated into the lateral pipeline after molded from plastic. The topside of the emitter clings to the inner wall of the pipe; the wall of the pipe near the emitter outlet is punctured through when integrating. Then the water can flow into the inlet of the emitter, flow around every tooth, and discharge from the outlet pore. The drip pipe with twenty-five emitters was installed in an experimental facility (figure 3). The measuring cups were used to collect the water discharged from the emitters in a given duration to calculate the flowrate of the emitters. Before the measuring, the air in the pipe was exhausted firstly, opened the valve little by little. When the pipe pressure remained in a steady condition, the static pressure from the manometer was recorded, as well as the duration and the amount of every emitter. The flow rate of the emitter at any given pressure was calculated from the average of the twenty-five emitters. Finally the COE curve can be made by regression analysis on the data.

It was very difficult to measure the pressure inside the flow path of the prototype emitters directly because of their tiny size. So an amplifying model of the emitter was manufactured with the dimension ratio 10:1 to verify the CFD modeling results of pressure distribution along the flow path (Wang, 2004). The amplifying model was made by steel and based on the similarity theory. Five pores with pressure tubes connected to manometers were made on the top wall of the amplifying emitter along the flow path. The pressures inside the flow path can be measured by the manometers.

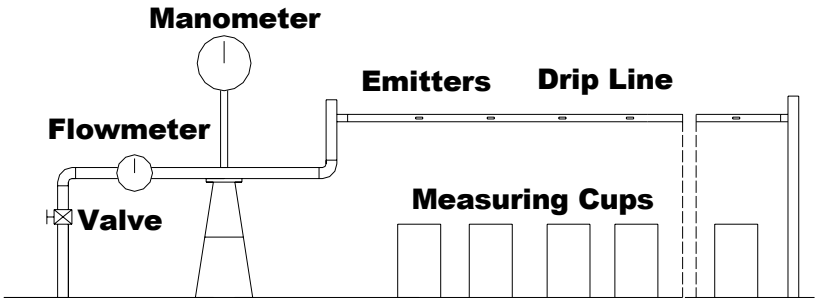

Figure 3. Schematic diagram of the experimental facility

Results and Discussions

COE comparison between CFD modeling and the measuring

Figure 4 shows the COE curves of prototype emitter and amplifying model made by regression analysis from the CFD modeling data and the measuring data. The broken curves are the CFD modeling results, and the continuous lines are the measuring results. It is showed that COE curves made by CFD modeling data are very close to that by measuring data, the CFD modeling results correlate well with the measuring results. The mean differences between the modeling results and the measuring results do not exceed 5 %. It is indicated that the COE can be numerically calculated by CFD method with high accuracy.

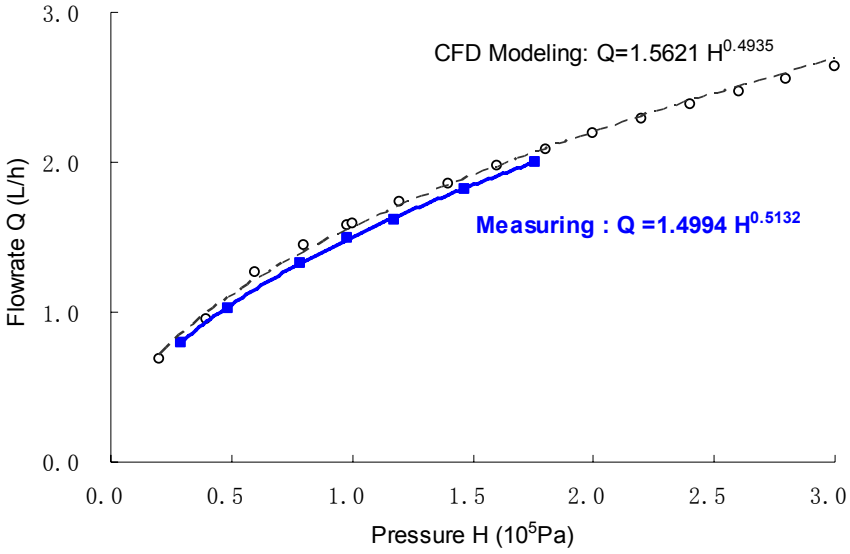

(a) Prototype emitters

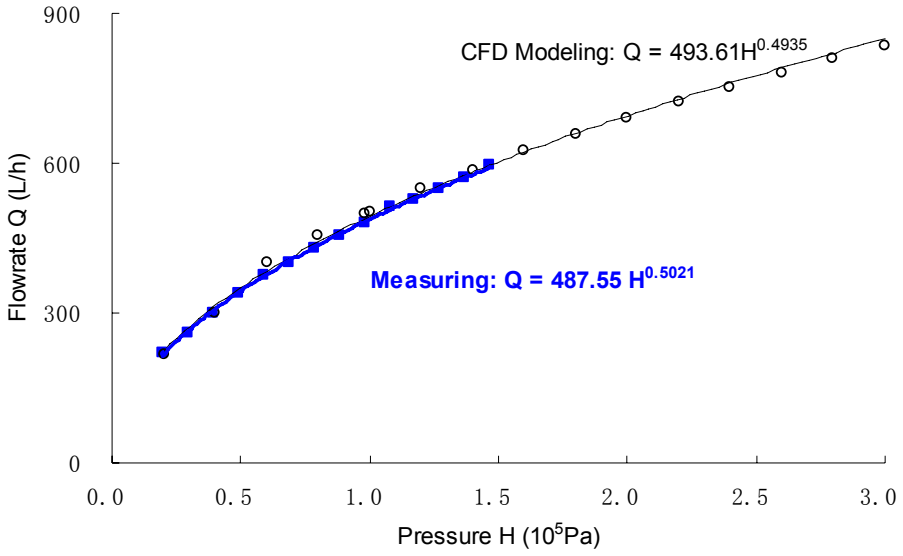

(b) Amplifying model

Figure 4. COE comparisons between the CFD modeling data and the measuring data (Broken line: CFD modeling; Continuous line: measuring)

Pressure distribution inside the flow path

The pressure distribution inside the flow path influences the hydraulic performance of the emitter greatly. Figure 5 a gives the pressure distribution inside the flow path of the emitter from the inlet to the outlet simulated by CFD method. The static pressure of the pipe was 10 m water head, the pressure unit in the legend was Pascal, and the grey level represents the pressure magnitude. The pressure in the left inlet area was higher than it was in the right outlet area, and reduced gradually from the inlet to the outlet. The detail pressure distribution between two teeth is given on figure 5 b. The direction of the arrow is the direction of the flow velocity of the position, and the white lines are the contour line of the pressure. The contour lines near the peak of the teeth were intensive, and the pressure gradient is very great there. When the water flows around the peak of the teeth, the flow direction is changed, and the flow pattern becomes unstable. So the structure and dimension of the peak of the teeth are very important to the hydraulic performance of the emitters; more attentions need to be paid to this aspect when designing a new emitter.

In order to further investigate the pressure distribution inside the flow path of the emitter, the pressures in sixteen positions along the flow path were numerically calculated by CFD method and were analyzed by standardized method. The pressure in every position was replaced by non-dimensional standardized pressure p_s, which was obtained by dividing the modeling pressure p_i in the position by the static pipe pressure p_P when modeling.

The standardized pressures p_s were only determined by the positions, so we can compare the

$$p_s = \frac{p_i}{p_P}$$

pressures with varying static pressure of the pipe. The standardized pressures by CFD modeling are shown with broken line on figure 6. The pressure decreases linearly with the length of the flow path. The pressures measured in the amplifying model at five positions are also shown with continuous line on figure 6. The pressures were also standardized by static pipe pressure when measuring. There is a linear regression relationship between the pressure and the length of the flow path with high coefficients of determination. The two regression curves by CFD modeling and by measuring are very close, and the average difference between the modeling pressure and the measuring pressure is no more than 3%. The pressure distribution modeling results agreed well with the pressure measuring results in amplifying model of the emitter.

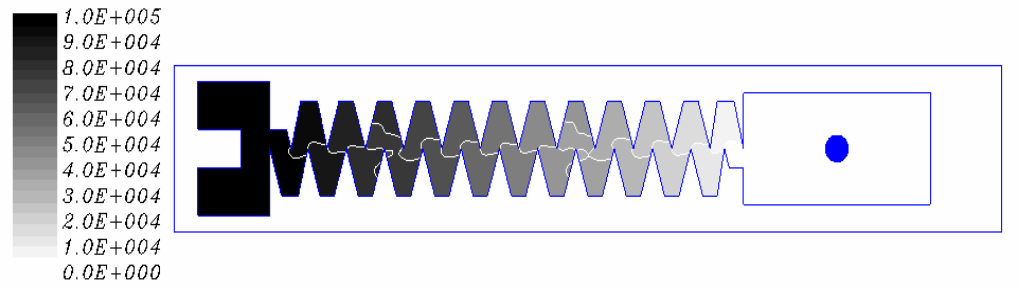

(a) Pressure distribution from the inlet to the outlet of the emitter

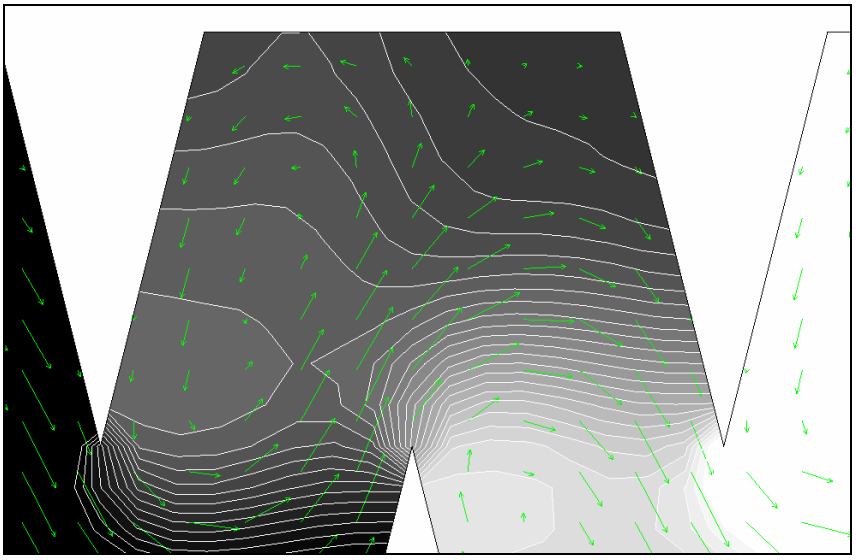

（b）Pressure distribution between the teeth

Figure 5. Pressure distribution inside the flow path of the emitter

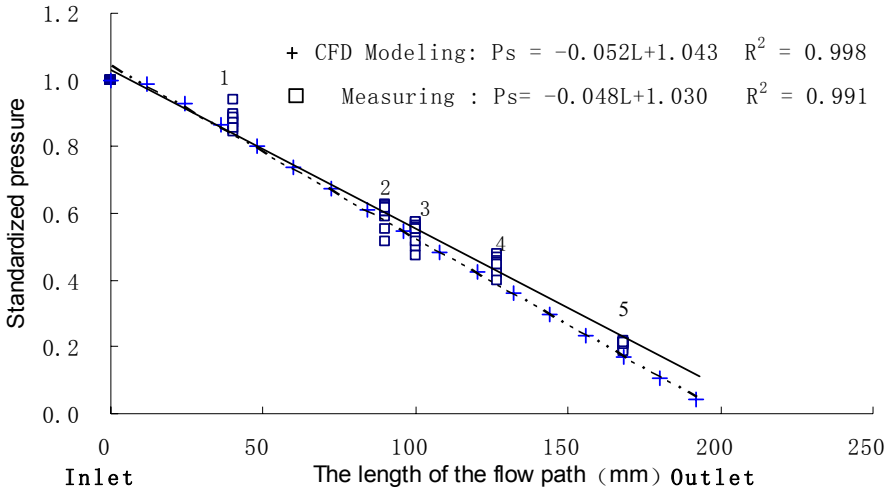

Figure 6. Standardized pressure curves comparison between CFD modeling and measuring

Flow velocity field inside the flow path

The flow field in the flow path of the emitters is very difficult to investigate by traditional methods. The flow velocity among the teeth by CFD modeling is shown on figure 7 a; the arrows are the velocity vectors in the flow field. It was found that the flow velocity near the peak of the teeth is much more than those at other places, a vortex is formed at the downstream side of the teeth, and the flow velocity in the area of the vortex is low. The vortex inside the flow path can improve the anti-clogging performance of the emitters because the vortex has a rinsing effect inside the flow path. A vortex is also formed in the outlet area of the emitter while the water discharge out the outlet pores (figure 7 b, c). The outlet area of the emitters in this study has a quadrilateral shape, and the water is stagnant in the four corners. The corner areas are easy to clog up if the irrigation water is not clean. The cylindrical outlet area would ameliorate the anti-clogging performance of the emitters; but it will require verification by experiments in future.

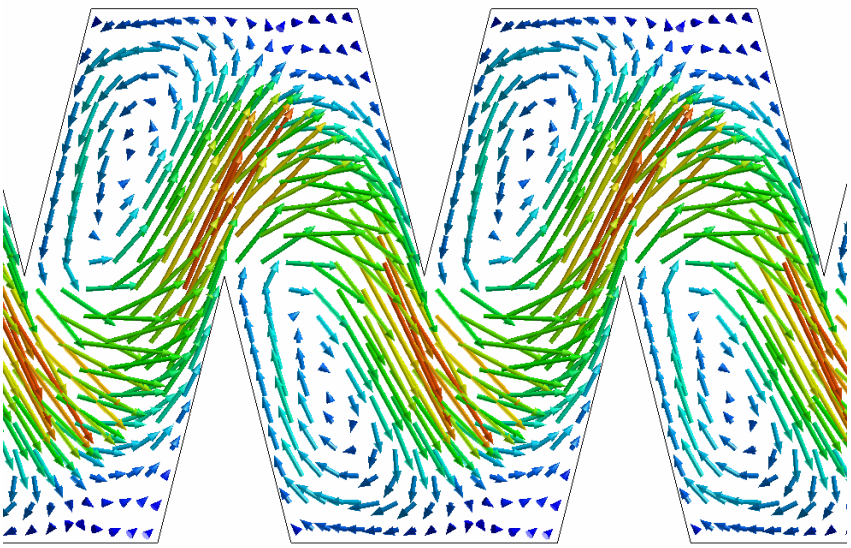

（a）Flow velocity vectors inside the flow path

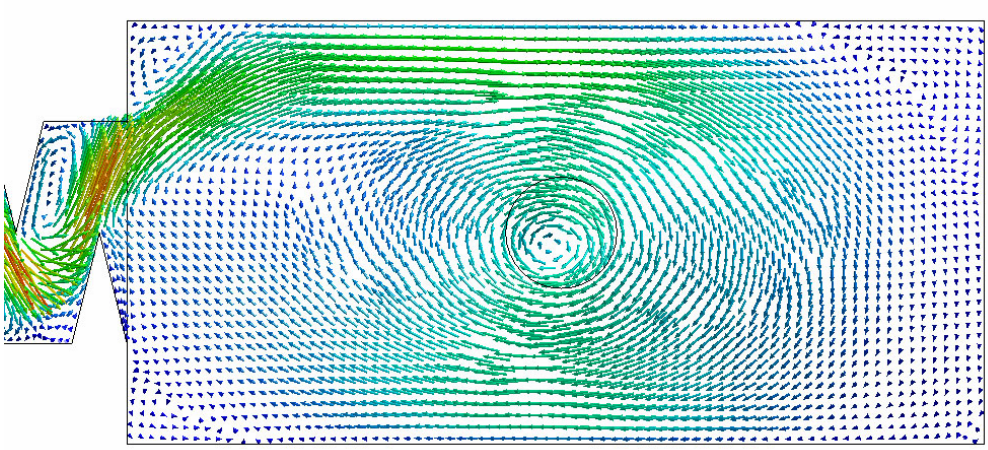

（b）Velocity distribution in the outlet area of the emitters

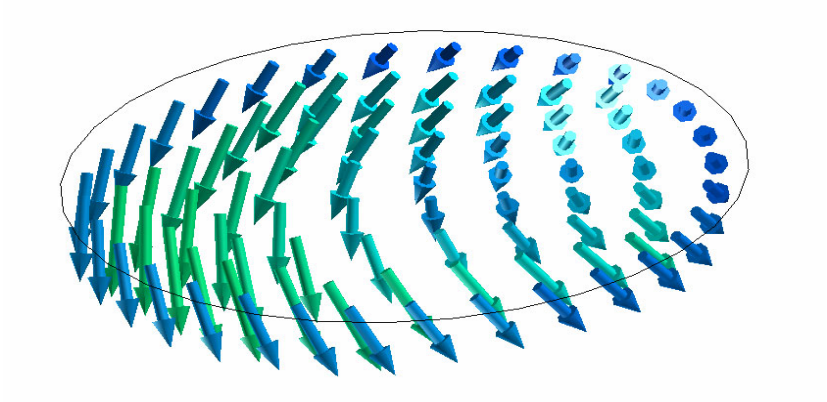

（c）Velocity vectors at the outlet pore of the emitters

Figure 7. Flow velocity field inside the flow path of the emitters by CFD modeling

Conclusions

1. The characteristics of the emitters (COE) were investigated by Computational Fluid Dynamics (CFD) method, and the modeling results were validated by measuring results in the laboratory. The CFD modeling results showed a good correlation with the measuring results; the average difference was no more than 5%. The CFD method was proved an effective method for the numerical calculation of COE with a high degree of accuracy.
2. The distributions of pressure and velocity in the flow path of the labyrinth emitter were numerically simulated by CFD method. An amplifying model of the labyrinth emitter was manufactured with dimension ratio 10:1 to verify the pressure distribution along the flow path. Both the modeling results and the measuring results indicated that the pressure was reduced linearly with the length of the flow path. The pressure distribution modeling results agreed well with the pressure measuring results in the amplifying model of the emitter. The average difference between the modeling results and the measuring results was no more than 3%.
3. The flow velocity near the peak of the teeth is much more than those at other place. A vortex is formed at the downstream side of the teeth, and the flow velocity in the area of the vortex was low. The vortex inside the flow path can improve the anti-clogging performance of the emitters because of rinsing effect.

Reference

1. Bennet, C. O., and J. E. Myers. 1995. *Momentum, Heat, and Mass Transfer*. New York, N.Y.: McGraw–Hill.
2. Fluent. 1998. *The user's Manual of Fluent*, version 6.1. Lebanon, N.H.: Fluent Inc.
3. Hinze, J. O. 1975. *Turbulence*, 2nd Ed. New York, N.Y.: McGraw–Hill.
4. I B, Short. T H. 2000. Two-dimensional numerical simulation of natural ventilation in a multi-span greenhouse. Transaction of ASAE*,* 43(3): 745 –753
5. John D., Anderson. *Computational Fluid Dynamics: The basics with application* [M].McGraw-Hill Inc, New York, 1995.
6. Karmeli D.1977. Classification and flow regime analysis of drippers. Journal of Agricultural Engineering Research 22:165-173.
7. Launder, B. E., and D. B. Spalding. 1974. The numerical computation of turbulent flows. Computer Methods in Applied Mechanics and Engineering 3: 269–289.
8. Palau Salvador, G. Arviza Valverde, J. Bralts, V. F. Hydraulic Flow Behavior through an In-line Emitter Labyrinth using CFD Techniques. 2004. ASAE/CSAE Annual International Meeting. Paper Number: 042252 Ottawa, Ontario, Canada, August 2004.
9. Wang, Jiandong. 2004. Study on the Hydraulic and Anti-clogging Performance of Emitters. Dissertation Paper. China Agricultural University. Beijing China.